Effects of Cyclic AMP on Fluid Absorption and Ion Transport Across Frog Retinal Pigment Epithelium

Measurements in the Open-Circuit State

BRET A. HUGHES, SHELDON S. MILLER, and TERRY E. MACHEN

From the Department of Physiology-Anatomy and the School of Optometry, University of California, Berkeley, California 94720

ABSTRACT A modified version of a capacitance probe technique has been used to measure fluid transport across the isolated retinal pigment epithelium (RPE)-choroid of the bullfrog. The accuracy of this measurement is 0.5–1.0 nl/min. Experiments carried out in the absence of external osmotic or hydrostatic gradients show that the RPE-choroid transports fluid from the retinal to the choroid side of the tissue at a rate of ~10 nl/min (4–6 $\mu l/cm^2 \cdot h$). Net fluid absorption (J_V) was abolished within 10 min by the mitochondrial uncoupler 2,4-dinitrophenol. It was also inhibited (70%) by the removal of bicarbonate from the bulk solutions bathing the tissue. Ouabain caused a slow decrease in J_V (no effect at 10 min, 70% at 3 h), which indicates that RPE fluid transport is not directly coupled to the activity of the Na-K pump located at the apical membrane of this epithelium. In contrast to ouabain, cyclic AMP (cAMP) produced a quick decrease in J_V (84% within 5 min). Radioisotope experiments in the open circuit show that cAMP stimulated secretory fluxes of Na and Cl, which accounted for the observed cAMP-induced decrease in J_V. The direction of net fluid absorption, the magnitudes of the net ionic fluxes in the open circuit, and the dependence of J_V on external bicarbonate concentration strongly suggest that fluid absorption is generated primarily by the active absorption of bicarbonate.

INTRODUCTION

In the vertebrate eye, the retinal pigment epithelium (RPE) is the major transport pathway responsible for the exchange of metabolites and ions between the choroidal blood supply and the neural retina (Noell, 1963; Steinberg and Miller, 1979; Miller and Steinberg, 1979, 1982). In the distal part of the neural retina, the extracellular space that surrounds the photoreceptor outer segments is called

Address reprint requests to Dr. Sheldon Miller, 360 Minor Hall, University of California, Berkeley, CA 94720.

J. GEN. PHYSIOL. © The Rockefeller University Press · 0022-1295/84/06/0875/25 $1.00

Volume 83 June 1984 875–899

the subretinal space. Sharing this space with the photoreceptors are the apical processes of the RPE cells. It has been shown that the ionic composition of this space can be altered by light and that these light-induced changes alter the electrical properties of the apical and basal cell membranes of the RPE (Oakley and Green, 1976; Oakley, 1977; Gold and Korenbrot, 1980; Griff and Steinberg, 1982; Linsenmeier and Steinberg, 1982; Linsenmeier et al., 1983).

The volume of fluid in the subretinal space helps determine the local concentration of ions and metabolites and therefore the electrical properties of the photoreceptors and PE cells (Capovilla et al., 1980; Miller and Steinberg, 1979, 1982; Steinberg et al., 1980). It is known that this space is filled with a matrix of material whose main chemical constitutents are mucopolysaccharides (Sidman, 1958; Berman, 1969; Bach and Berman, 1971; Feeney, 1973). The hydrophilic nature of these molecules may be an important component of the mechanism that controls the hydration and volume of the subretinal space. Another important factor might be solute-linked fluid transport by the RPE, but up to the present there have been no direct measurements of fluid tranpsort across the isolated RPE.

The goal of the present experiments was to measure directly the fluid transport across the isolated RPE and to ascertain its magnitude and direction, in the absence of external hydrostatic and osmotic gradients. Since water transport is usually coupled to the active transport of ions, we also measured the isotopic fluxes of Na, K, and Cl in the open circuit. This is the condition in which fluid transport is measured and which is most nearly comparable to the in vivo situation.

The present experiments show that fluid is transported across the isolated bullfrog RPE-choroid from the retinal to the choroidal side of the tissue at a rate of 4–6 $\mu l/cm^2 \cdot h$. This fluid transport is reduced by metabolic inhibitors and cyclic AMP (cAMP). Ionic flux measurements show that active bicarbonate transport, followed by passive Na and K movement, provides the main driving force for the fluid absorption.

A preliminary account of some of this work has previously been presented in abstract form (Hughes et al., 1982) and in a short report (Miller et al., 1982).

MATERIALS AND METHODS

Bathing Media

In most experiments, the composition of the normal Ringer's solution was (in mM): 82.5 NaCl, 27.5 $NaHCO_3$, 2.0 KCl, 1.0 $MgCl_2$, 1.8 $CaCl_2$, 10 glucose; it was gassed with water-saturated 95% O_2/5% CO_2 to a pH of 7.4 ± 0.1. The osmolarity of this solution was 227 mosmol. Phosphate-buffered Ringer's, gassed with 100% O_2, was used to determine the effect of bicarbonate removal on fluid transport. It had the following composition (in mM): 82.5 NaCl, 27.5 Na gluconate, 2.0 KCl, 0.375 NaH_2PO_3, 2.125 Na_2HPO_3, 1.0 $MgCl_2$, 1.8 $CaCl_2$, 10.0 glucose. The pH of this Ringer's was 7.4 ± 0.1.

In some experiments, the effects of certain drugs on fluid transport were tested. Ouabain, 2,4-dinitrophenol, cAMP, dibutyryl cAMP (dbcAMP), 3-isobutyl-1-methylxanthine (IBMX), Na azide, and iodoacetamide were obtained from Sigma Chemical Co., St.

Louis, MO. All were added from stock solutions in volumes of 600 μl to the apical bathing solution of the water flux chamber.

Dissection

Medium-sized bullfrogs (Central Valley Biologicals, Clovis, CA) were kept in running tap water at 19.0°C on a photoperiod of 12 h dark/12 h light for at least 2 d before use. The RPE-choroid was dissected from the eyes of dark-adapted frogs under dim red light as described previously (Miller and Steinberg, 1977*a*).

Isotopic Fluxes

The measurement of unidirectional fluxes was carried out as described in the previous paper (Miller and Farber, 1984), but in this case transepithelial potential (TEP) was continuously monitored and no short-circuit current was applied.

Fluid Transport

TISSUE MOUNTING Pieces of the RPE-choroid, ~50 mm^2, were carefully draped, choroid side down, over 10-mm-diam disks of either nitrocellulose microporous filter (effective pore diameter 0.8 μm; Amicon Corp., Lexington, MA) or nylon fabric (HC 3-209; Tetco, Inc., Elmsford, NY). No difference in the results was seen using either disk. The disks supported the tissue during the mounting procedure and prevented it from bowing while the chamber was filled with bathing solution. The hydraulic conductivity of the microporous filter is >1 cm/s·atm and that of the nylon mesh is undoubtedly higher since it has 57% open area. Therefore, these supports do not create a significant barrier to fluid transport across the RPE.

WATER FLUX CHAMBER Fluid transport (J_V) across the RPE-choroid was measured in a specially designed chamber built entirely of Kel-F, a water-impermeable plastic (Fig. 1). This material was a generous gift of Ted Knudsen (Fluorocarbon Co., Anaheim, CA). Chambers built of other plastics, such as Lucite, absorb fluid at rates that are comparable to the flow generated by the tissue itself. These materials therefore limit the resolution of the volumetric fluid transport measurement (Fischbarg and Whittembury, 1978; Welsh et al., 1980).

The RPE is extremely delicate and special precautions must be taken to minimize the extent of edge damage that is the inevitable consequence of mechanical sealing. We used a mounting chip that was designed to compress uniformly the tissue in a reproducible manner (see Fig. 1, inset). The RPE-choroid and support were placed in the recess of the holding plate (*A*), and the sealing disk (*B*) was then set into this recess over the tissue and tightened down by a pair of machine screws. Both the plate and sealing disk had central apertures that exposed 0.126 cm^2 of the tissue to the bathing solutions. The sealing disk also had a compartment, ~150 μm deep, which was designed to accommodate without compression the tissue plus its support when the disk was firmly screwed into the holding plate. The seal around the circumference of the disk was achieved by a pair of 0.5-mm-wide ridges that encircled the central aperture; the inner ridge (*C*) extended down ~50 μm from the base of the disk's recess and the outer ridge (*D*) extended down from the recess by ~100 μm. This configuration produced two bands of compression that sealed the edge of the tissue without causing damage to the areas lying outside the sealing ridges.

The mounting plate was clamped between identical Kel-F half-chambers so that the apical side of the tissue could alternatively face the right or left half-chamber. This design feature was used to eliminate systematic errors in the J_V measurement that might arise from differences in the background volume changes of the two half-chambers (see control

section below). The half-chambers were made by a two-piece construction consisting of a main body (*E*), an end plug (*F*) that served to seal both the back of the chamber, and a water jacket (not shown). In addition, the end plug held various transducers that are described below.

The presence of air bubbles can cause small fluctuations in the volume of the bathing solutions that may impinge on the volumetric determination of fluid transport across

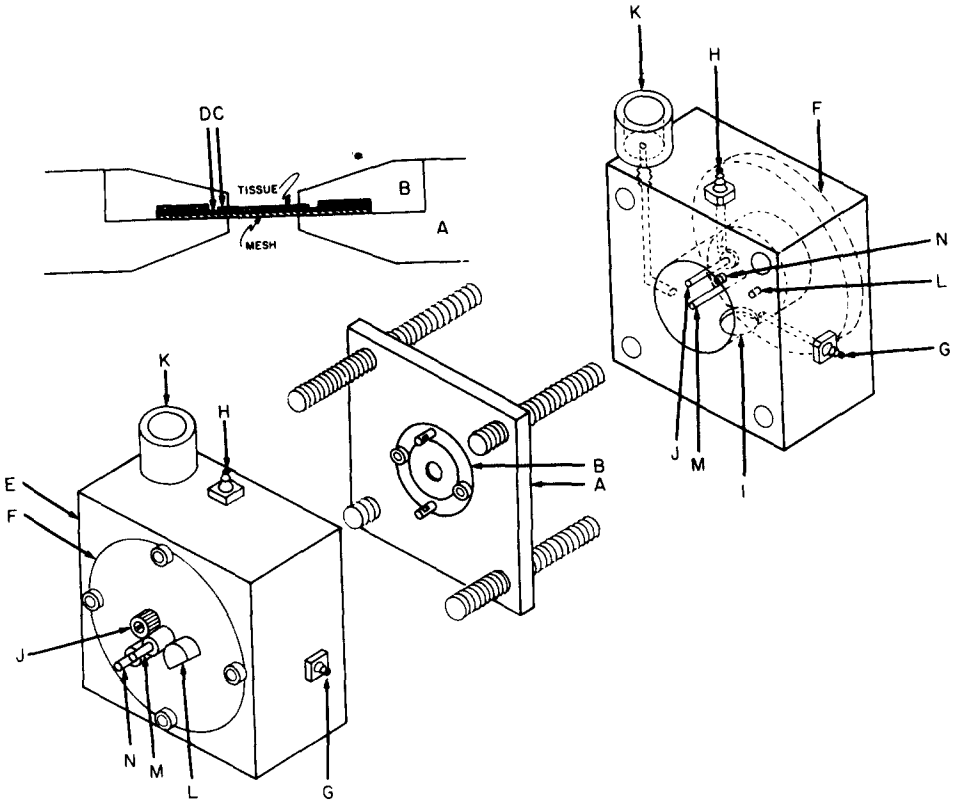

FIGURE 1. Schematic representation of the Kel-F chamber used in fluid transport measurements across the RPE-choroid. *A*, tissue-holding plate; *B*, sealing disk; *C* and *D*, compression ridges; *E*, half-chamber body; *F*, end plate; *G*, inlet; *H*, outlet; *I*, well for magnetic stirring bar; *J*, thermistor; *K*, Teflon cup; *L*, calibration screw; *M*, PD-sensing electrode; *N*, current-passing electrode. Inset: cross section of tissue mount.

epithelia. In order to prevent the adhesion of air bubbles to the chamber walls, the cavity surfaces were thoroughly cleaned with absolute ethanol before filling the chambers with bathing media. In addition, it was necessary to apply a small amount of a wetting agent (diocyl Na-sulfosuccinate) to the upper corner formed by the junction between the cavity wall and the end plate. Consequently, there was a small quantity of surfactant in the bathing media ($<10^{-7}$ M), which did not have any deleterious effect on the tissue as judged by the TEP and R_t.

The half-chambers each held ~12 ml of solution and were filled simultaneously using

push-pull syringes (not shown). Polyethylene tubing was used to connect the syringes to stainless steel fittings of the inlet (*G*) and outlet (*H*) of each half-chamber. These push-pull syringes were used for complete solution changes as well as for the initial chamber filling. Three-way miniature valves (Hamilton Co., Reno, NV), located ~1 cm away from the chamber ports, served to open the half-chambers to the push-pull syringes or to close them off completely.

The bathing solutions could not be bubbled with O_2 during the course of the experiments. Given the relatively large volume of the bathing solutions (24 ml), there should be ample O_2 available to keep even a tissue with high O_2 demands alive for hours. At 20°C, there is ~30 μmol of O_2 in 24 ml of a Ringer's solution that is equilibrated with 95% O_2/5% CO_2. If we assume that the bullfrog RPE has an O_2 consumption rate of 80 nmol/$cm^2 \cdot h$, equal to that of the rabbit corneal epithelium (Freeman, 1972), then a piece of tissue 0.126 cm^2 in area would consume O_2 at a rate of ~10 nmol/h. Thus, in 5 h, only 50 nmol or 0.2% of the O_2 in the bathing media would be consumed.

The bulk solutions were mixed by Teflon-coated magnetic stirring bars that rested in depressions located on the bottom of each half-chamber (*I*); these stirring bars were driven by magnets that were attached to DC motors and positioned beneath the half-chambers. The solutions were not stirred continuously because in some preparations this was found to cause an irreversible drop in the TEP.

Since changes in the temperature of the bathing solutions result in volume changes caused by thermal expansion properties of water, it is important to regulate the temperature of the bathing medium within narrow limits. A change in the temperature of 12 ml of water from 19.0 to 19.1°C will produce a volume increase of ~240 nl, which may be large relative to the magnitude of the volume change resulting from fluid transport across the tissue. The temperature of the bathing solutions was regulated by circulating thermostatically controlled water (±0.03°C) via a circulator (K-2/R; Lauda Div., Brinkmann Instruments, Inc., Westbury, NY) through the water jackets that surrounded the cavity of each half-chamber. This maintained the temperature of the bathing solutions at 19 ± 0.1°C; small fluctuations in the temperature of the bathing medium sometimes occurred after changes in ambient temperature and brief periods of stirring the bulk solutions, but these changes were equal in both half-chambers and had no discernible effect on the water flux measurement (refer to section on controls). The temperature of the bathing medium was monitored on both sides via Yellow Springs 402 thermistors (Yellow Springs Instrument Co., Yellow Springs, OH) in conjunction with a Yellow Springs 43TD two-channel telethermometer and recorded on a three-channel strip-chart recorder (Soltec Corp., Sun Valley, CA). The thermistors were imbedded in heat-sink compound and contained in stainless steel cases that extended into the bathing solutions from the ends of the half-chambers (*J*).

In the process of adding drugs, it was important to minimize perturbations in the temperature of the bathing solutions for the reasons discussed above. We therefore adopted the following protocol: after J_V had reached a steady state rate, 600 μl of Ringer's containing the drug, cooled to about 10°C, was introduced onto the bottom of the half-chamber in exchange for an equal amount of "old" Ringer's using a small pair of Kel-F push-pull syringes. In control experiments, we used a single half-chamber sealed with a Lucite window to show that when solution marked with a small amount of dye was introduced into the chamber, it layered almost completely in the stirring well, with no apparent mixing into the bulk solution. The introduction of the concentrated drug solution sometimes caused a transient change in the apparent volume flow across the tissue, but this artifact was usually complete within 5 min. After J_V returned to steady state levels, the layered drug was mixed into the bathing solution by turning on the

stirring bars for 15 s. In control experiments, this was found to be sufficient time to mix completely a dye that was layered on the bottom of the half-chamber into the bulk solution.

FLUID TRANSPORT MEASUREMENTS Fluid transport was measured using the volumetric technique developed by Wiedner and his colleagues (Wiedner, 1976; Wright et al., 1977; van Os et al., 1979). Each half-chamber had a smooth-walled Teflon cup fixed to its top (*K*). Each cup was partially filled to approximately the same level with Ringer's solution continuous with the solution in the half-chamber via 1-mm-diam, L-shaped channels. The level of solution in each cup was monitored continuously by commercially available capacitance-measuring probes and associated amplifiers (Mechanical Technology, Inc., Latham, NY). These probes measured the capacitance of the air gap between the surface of the probe and the surface of the solution. A change in the volume of the bathing solution alters the height of the meniscus in the cup and causes a proportional change in the output of the amplifier. The outputs of the probe amplifiers were recorded individually and differentially on a three-channel strip-chart recorder (E+K Scientific Instruments, Saratoga, CA).

The probes were aligned over the cups by support columns fixed to a base that also held the chamber (not shown) and could be lowered or raised by micromanipulators. The base had adjustment screws in each corner that were used to level the apparatus. Evaporation of fluid from the cups was reduced by Kel-F covers that had central holes through which the probes fit.

The probes were calibrated by separating the half-chambers with a blank Kel-F plate and displacing 0.25–3 μl of the bathing solutions by rotating calibration screws located in the half-chamber end pieces (*L*). For each microliter of volume change, there was a 600-mV change in the probe amplifier output. This relationship held for both probes whether the calibration screws were advanced or retracted. When this procedure was repeated with a piece of RPE-choroid plus either a micropore filter or a nylon screen mounted in the holding plate, the ratio of the probe output change to the volume displacement was again found to be 600 mV/μl. This means that the compliance of the tissue and its support was sufficiently low, such that there were no volume changes caused by tissue bowing when microliter changes in volume were made. We used this ratio in subsequent calculations of volume changes.

Transepithelial resistance (R_t) is one measure of the effectiveness of the mechanical seal on the RPE. A relatively low R_t is one indicator of the damage that the RPE can incur during dissection or when it is clamped in the holding plate. It has been previously shown that net isotope fluxes could not be reliably measured unless the R_t of the bullfrog RPE was >250 $\Omega \cdot cm^2$ (Miller and Steinberg, 1977*a*). Regions of tissue damage in these preparations could conceivably provide a pathway of high hydraulic conductivity through which passive volume flow might occur if the solutions in the Teflon cups are at slightly different levels. During the course of the experiment, we routinely tested for paracellular leaks by applying a hydrostatic pressure gradient of 2–4 mm H_2O opposite to the direction of fluid transport. In most tissues with resistances of <300 $\Omega \cdot cm^2$ at $t = 60$ min, this maneuver resulted in a significant reduction in the magnitude of J_V and sometimes caused a reversal of its direction. Data obtained from these tissues were rejected. In contrast, in tissues of resistance >300 $\Omega \cdot cm^2$, J_V was unaffected by these small hydrostatic pressure gradients.

The resolution of the volumetric technique is limited by "background volume changes" (E_A and E_B; see below) that occur in both half-chambers. In principle, these volume changes may result from evaporation, thermal expansion and contraction of both the chamber and the bathing solutions, leaks, and fluid absorption by the chamber materials. An accurate measurement of fluid transport cannot be made if the background volume

changes are significantly different in the two half-chambers. The Kel-F chamber was specifically designed to minimize these factors and an extensive series of control experiments was carried out to determine the magnitude of the background volume changes. It is important to note that a sufficiently high resolution in these measurements can be obtained even if the rate of background volume change exceeds the rate of fluid transport by the epithelium. This resolution is possible because the volume changes are monitored on both sides of the tissue, and the background changes, if equal, can be subtracted out of the voltage signal from each half-chamber. Assuming volume conservation and absorption of fluid across the tissue, the rate of volume change in each half-chamber will be

$$\begin{aligned} A &= E_A - J_V \\ B &= E_B + J_V, \end{aligned} \tag{1}$$

where A is the total rate of volume change on the apical side; B is the total rate of volume change on the basal side; E_A is the rate of background volume change on the apical side; E_B is the rate of background volume change on the basal side; and J_V is the net fluid transport from the apical to the basal side of the epithelium.

If the rate of background volume change is the same for both half-chambers, i.e., $E_A = E_B$, then the rate of fluid transport is

$$J_V = (A - B)/2. \tag{2}$$

In order to determine E_A and E_B, we mounted a sheet of parafilm in the holding plate and measured the volume change of the solution in each half-chamber as a function of time. The results of one such experiment are shown in Fig. 2*A*. In this figure, the slopes of the lines labeled A and B must represent the background volume changes E_A and E_B since J_V, by design, is zero.

The time course of the volume decrease in both half-chambers reveals two phases. In each case, the "transient" phase (0–50 min) parallels the time course of the thermal equilibration of the Ringer's (23°C) with the water jacket (19°C), and is characterized by a monotonically decreasing slope. One can calculate that 12 ml of water, cooled from 23 to 19°C, will contract by ~10 μl. This calculated value coincides with the observed volume decrease that occurs between 0 and 50 min. Therefore, the initial phase of volume decrease, the transient, is most likely a reflection of the thermal contraction of the bathing medium.

In the second phase, there is a steady state rate of volume loss that is ~20 nl/min from each half-chamber (average ± SD = 21.5 ± 5.0, $n = 70$). In this experiment (Fig. 2*A*), the apparent J_V ($t > 50$ min), according to Eq. 2, would be zero, as evidenced by the slope of the A − B trace. The steady state phase of background volume loss is due to evaporative fluid loss from the Teflon cups, since in separate experiments this rate was found to be directly related to changes in ambient temperature and humidity.

The rate of baseline volume change was regularly assessed in parafilm control experiments that were conducted before and after experiments involving the RPE. The time course of the apparent J_V for eight such parafilm experiments is summarized in Fig. 2*B*. There was much variability in the baseline J_V during the period that corresponds to the temperature equilibration of the bathing solutions, as can be seen from the size of the standard error bars at $t = 20$ min. The variability was even greater at earlier times (not shown). This variability was probably the result of the frequently observed difference between the rates at which the bathing media in each half-chamber cooled. After 40 min of equilibration, however, the apparent J_V across the parafilm at any given time was zero. These parafilm data show that J_V can be accurately measured across epithelia without interference from background volume changes.

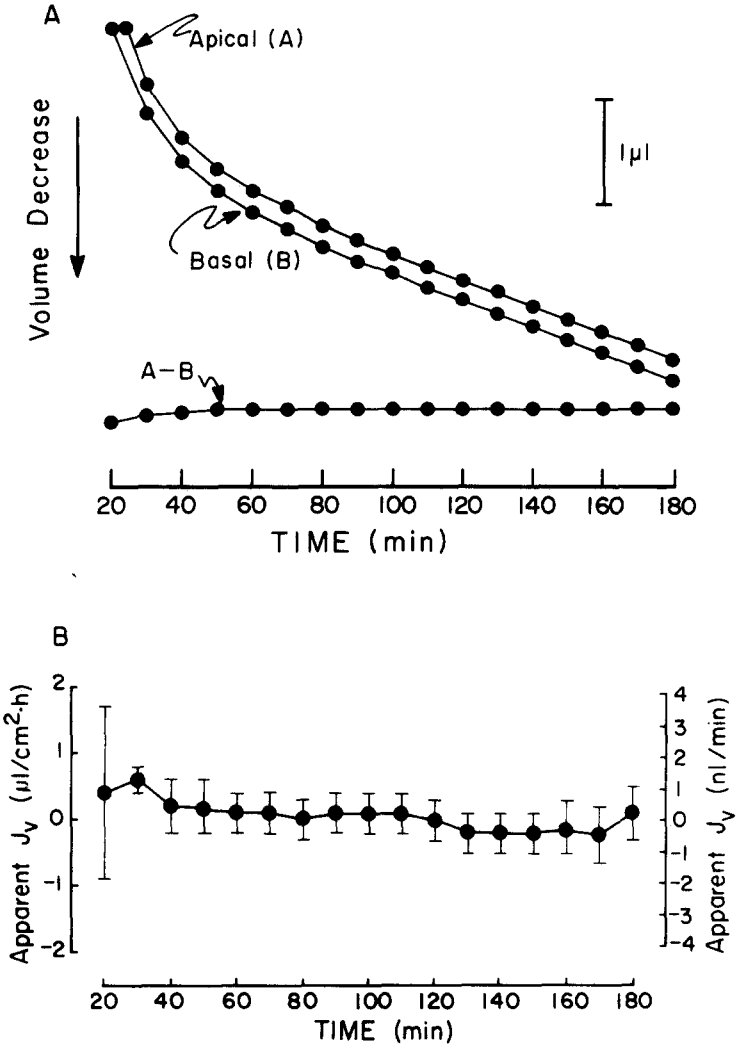

FIGURE 2. (*A*) Parafilm control experiment showing the time course of baseline volume changes of the solutions in the "apical" and "basal" half-chambers. The lower trace represents the difference between the rates of volume decrease on the two sides. Normal Ringer's, ≈23°C, was introduced into the half-chambers at $t = 0$ min. After a period of ~50 min, the volume decreases in the two half-chambers reached identical, steady state rates of ~20 nl/min. This corresponded with the time it took for the solution to thermally equilibrate with the water jacket temperature (19°C). (*B*) Time course of apparent J_V across a sheet of parafilm. Each point and vertical bar represents the mean ± SEM of seven to eight experiments. The ordinate on the left shows the apparent J_V normalized for surface area; the ordinate on the right shows the apparent J_V in absolute units. At times <20 min, the apparent J_V was highly variable because of the thermal equilibration of the bathing solutions. These controls either preceded or followed experiments involving the RPE.

ELECTRICAL MEASUREMENTS IN THE WATER FLUX CHAMBER The TEP was measured using agar-Ringer bridges and Ag-AgCl electrodes connected to a high-impedance voltmeter. The Ringer bridges and electrodes were encased in Kel-F tubes that were press-fitted through the end piece of each half-chamber (*M*); this positioned the tips of the bridges ~2 mm away from either side of the tissue. Electrode asymmetry (usually <1 mV) was compensated for by an internal bucking device. The low impedance of the RPE-choroid made it possible to use one of the electrodes simultaneously as a reference for the TEP measurement and as a ground return for the two capacitance probes.

We used a current clamping device to measure R_t at roughly 10-min intervals by passing 1-μA current pulses via Ag-AgCl electrodes located at the end of each half-chamber (*N*) and recording the resulting change in potential difference. The resistance of the bathing solutions and the nylon screen or microporous filter were corrected for in the determination of R_t.

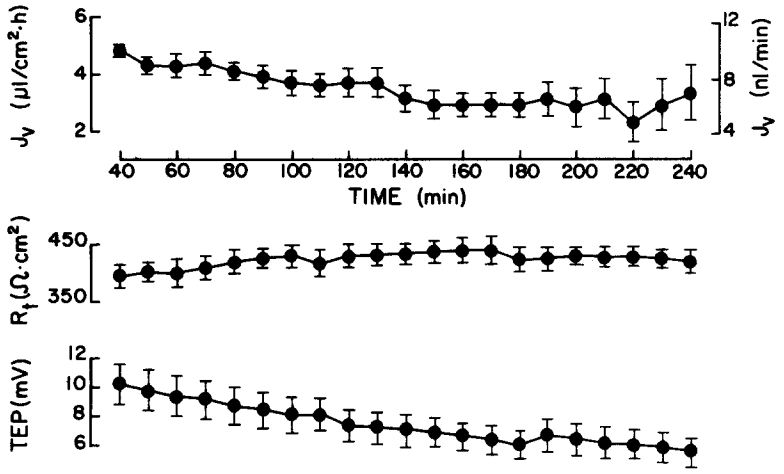

FIGURE 3. J_V, R_t, and TEP across the RPE-choroid as a function of time. Each point and vertical bar represents the mean ± SEM of five to eight experiments. The ordinate on the left shows J_V normalized for surface area; the ordinate on the right shows J_V in absolute units. R_t and TEP at $t = 0$ were 298 ± 17 Ω·cm² and 12.8 ± 1.9 mV, respectively.

RESULTS

Direction and Rate of Fluid Transport

Fig. 3 is a summary of the results from seven experiments in which the RPE-choroid was bathed on both sides with identical bicarbonate Ringer's (Materials and Methods). The average rate of fluid transport, J_V, was 4.3 μl/cm²·h after 50 min of thermal equilibration. In every experiment, fluid was transported from the apical to the basal side of the epithelium and this fluid absorption continued for ≥4 h.

Fig. 3 also shows the time course of J_V, TEP, and R_t. Relative to J_V at $t = 60$ min, J_V decreased at a rate of 16.3%/h. The average TEP at $t = 0$ was 12.8 ±

1.9 mV (mucosa positive) in this group of tissues. After 60 min of equilibration, TEP had dropped to 9.4 mV, and relative to this value, a slow decrease was observed (14%/h). R_t started at 298 ± 17 $\Omega \cdot cm^2$, increased to 400 $\Omega \cdot cm^2$ by t = 60 min, and changed little thereafter.

Effects of Dinitrophenol on J_V

The driving force for net fluid transport cannot be due to a difference in osmolarity between the external bathing solutions since the tissues are bathed on both sides with identical Ringer's, and it cannot be hydrostatic since net fluid is absorbed even in the presence of opposing hydrostatic heads (Materials and Methods). Since net fluid absorption is not passively driven, we examined the effect of some inhibitors of cell metabolism.

In Fig. 4*A*, the difference trace, A − B, shows that the mitochondrial uncoupler 2,4-dinitrophenol (DNP) can quickly decrease the rate of fluid transport to zero. The average slope of this difference curve, which equals $2J_V$ (Eq. 2), is 8 $\mu l/cm^2 \cdot$ h before the addition of DNP ($t < 100$ min) and 0 $\mu l/cm^2 \cdot h$ after addition of DNP ($t > 100$ min). Therefore, 1 mM DNP, added to the solution on the apical side of the tissue, reduced J_V from 4 to 0 $\mu l/cm^2 \cdot h$.

Fig. 4*A* also shows the effect of DNP on the rate of volume decrease in the solutions bathing the apical (A) and basal (B) sides of this tissue. The total rate of volume decrease is the sum of the rate of evaporative fluid loss and the rate at which fluid is transported into or out of the half-chamber (Eq. 1). There was a net decrease in the volumes throughout the course of the experiment because of the relatively high rate of evaporative fluid loss from the Teflon cups. From 50 to 70 min, the rate of volume decrease was greater on the apical side than on the basal side, as can be seen from the slopes of the respective lines. This indicates that there was fluid transport across the tissue from the apical to the basal half-chamber. We assume from the parafilm experiments that the rate of background volume change is the same in both half-chambers, $E_A = E_B$ (Fig. 2), and therefore the slope of the difference trace is a direct measure of the rate of fluid transport (4 $\mu l/cm^2 \cdot h$).

Between 70 and 90 min, 600 μl of a concentrated solution of DNP was slowly layered onto the bottom of the apical half-chamber in exchange for 600 μl of "old" Ringer's using the small push-pull syringes. This maneuver had little effect on J_V because of the long diffusion path separating the tissue from the DNP (~0.5 cm). At 100 min, the solutions on both sides were stirred for 15 s, which raised the concentration of DNP in the apical solution to 1 mM. This immediately decreased the rate of fluid absorption.

FIGURE 4. *(opposite)* (*A*) Effect of DNP on the rates of volume decrease of solutions bathing the apical and basal sides of an RPE preparation. The lower trace represents the difference between the rates measured on the two sides. (*B*) Effect of DNP on J_V, R_t, and TEP across the RPE-choroid. Each point and vertical bar represents the mean ± SEM of seven experiments. J_V has been normalized to percent initial rate; the mean initial J_V was 4.1 ± 0.9 $\mu l/cm^2 \cdot h$. The time required for J_V to reach a steady state varied from tissue to tissue, and thus the time scale, have been normalized to the time at which the drug was mixed into the bathing solution.

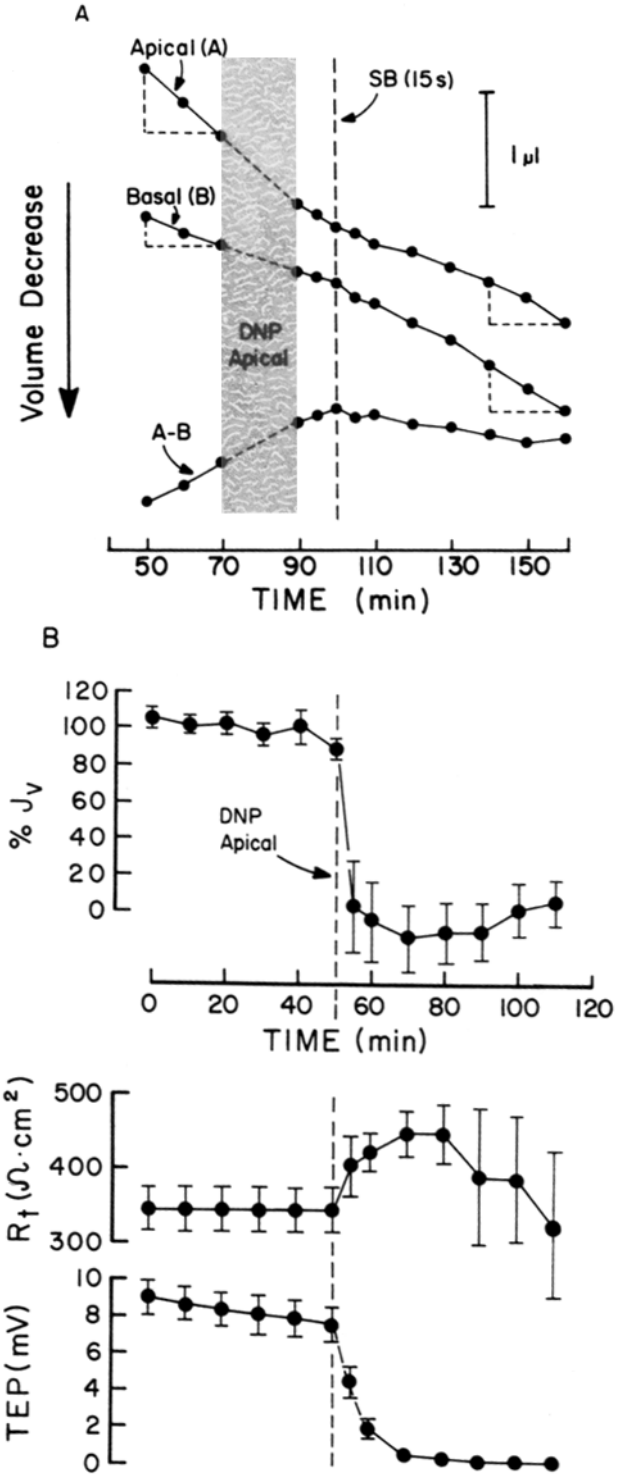
A
Apical (A)
SB (15 s)
1 µl
Basal (B)
Volume Decrease
DNP
Apical
A-B
50 70 90 110 130 150
TIME (min)
B
120
100
80
60
40
20
0
% J_V
DNP
Apical
0 20 40 60 80 100 120
TIME (min)
500
400
300
R_t ($\Omega \cdot cm^2$)
10
8
6
4
2
0
TEP (mV)

From the slopes of the lines, we can see that the rates of volume decrease between 140 and 160 min are equal on the two sides. This is what one would expect if DNP completely inhibited the active transport processes responsible for generating J_V. The slope of these lines is ≃20 nl/min, which is equal to the background volume losses (E_A, E_B) measured in the parafilm control experiments (Fig. 2*A*). This finding helps validate the use of the difference trace as a direct measure of J_V.

Previous investigators, working with other epithelia, have estimated J_V by measuring volume changes on only one side of the tissue (Fischbarg and Whittembury, 1978; Welsh et al., 1980). It is important to note that the variability of the background volume changes observed in our chamber system, 2 SD = 10 nl/min, is comparable to the rate of fluid transport. Therefore, it would be difficult, in the RPE, to estimate the magnitude or direction of fluid transport from volume measurements on only one side of the tissue.

Fig. 4*B* summarizes the results of six DNP experiments (100% J_V corresponds to 4.1 ± 0.9 $\mu l/cm^2 \cdot h$). In each experiment, DNP (1 mM) caused a rapid decrease in J_V. Within 5 min, the rate of fluid absorption dropped to a value indistinguishable from zero. There was an indication of a small amount of fluid secretion between 60 and 90 min since the mean was negative, but it was not statistically significant.[1]

Fig. 4*B* also shows that the average R_t in these tissues was 343 $\Omega \cdot cm^2$ immediately before treatment of the tissue with DNP. DNP caused R_t to increase by ~100 $\Omega \cdot cm^2$. In two of the tissues, the resistance began to fall after 30 min of exposure, but not before the fluid transport had been completely abolished. DNP caused a monotonic decrease in the TEP immediately after it was mixed into the apical solution.

In addition to DNP, the effect of some other metabolic inhibitors was investigated. In one experiment, the normal, oxygenated Ringer's bathing the RPE-choroid was replaced with normal Ringer's gassed with 95% N_2/5% CO_2 and containing 1 mM iodoacetamide. After 4 h, J_V dropped from 4.6 to 0 $\mu l/cm^2 \cdot h$, TEP decreased from 9.5 to 0.2 mV, and R_t decreased from 300 to 30 $\Omega \cdot cm^2$. In spite of the low resistance at the end of the experiment, the tissue was apparently well sealed since it held a hydrostatic pressure difference of 5 mm H_2O with no apparent fluid leak. In two other experiments, 1 mM Na azide and 1 mM iodoacetamide were mixed into the apical solution. After 2 h, J_V decreased from 4.1 to 0.5 $\mu l/cm^2 \cdot h$ in one experiment and from 11.0 to 1.6 $\mu l/cm^2 \cdot h$ in the other. Concomitantly, TEP decreased from 13.0 to 2.2 mV and from 10.4 to 2.4 mV, and R_t changed from 315 to 340 $\Omega \cdot cm^2$ and from 340 to 250 $\Omega \cdot cm^2$.

[1] J_V has been normalized to percent of the initial rate of absorption because of the tissue-to-tissue variability. The time scale has also been normalized such that the point when the drug was mixed into the apical bathing solution is arbitrarily set at t = 50 min. This normalization was made because some tissues took slightly different times (±10 min) to reach the steady state and the drug was always mixed into the apical solution after fluid transport had proceeded at a steady state for 50 min. In addition to the criterion of $R_t \geq 300\ \Omega \cdot cm^2$ at t = 60 min, acceptable tissues had steady state spontaneous rates of decline of J_V no greater than 20%/h.

Effect of Bicarbonate Removal on J_V

Fluid transport across epithelia, in the absence of external osmotic and hydrostatic gradients, has been shown to be coupled to active salt transport wherever it has been studied (House, 1974). From tracer flux studies in the short-circuited state, it has been inferred that the RPE actively absorbs bicarbonate (Miller and Farber, 1984). In the open circuit, bicarbonate is the only major ionic species to exhibit net transport against its transepithelial electrochemical gradient (see Discussion). Since this net bicarbonate flux is absorptive, it most likely provides the driving force for fluid absorption.

Table I shows the effect of replacing bicarbonate Ringer's (27.5 mM) with phosphate-buffered Ringer's in which bicarbonate has been replaced with gluconate. Bicarbonate removal resulted in a 70% decrease in the rate of fluid absorption. Although the residual J_V may result from the presence of other driving forces, it should be noted that the magnitude of this flux (1.4 ± 0.7 $\mu l/cm^2 \cdot h$) relative to the baseline, as determined by the parafilm controls (Fig. 2*B*), is not statistically significant ($P = 0.17$; t test).

TABLE I

Effect of Bicarbonate Removal on J_V

	J_V	TEP	R_t
	$\mu l/cm^2 \cdot h$	mV	$\Omega \cdot cm^2$
Bicarbonate Ringer's*	3.9±0.4	9.8±0.4	328±20
Bicarbonate-free Ringer's*	1.4±0.7	6.2±0.4	313±25
Percent decrease	70±16	—	—

* Mean ± SEM, $n = 8$.

The value in each column refer to means ± SEM for eight tissues. Row 1 shows J_V, TEP, and R_t values from tissues bathed in bicarbonate Ringer's. Row 2 shows steady state values from the same tissues after they were bathed in nominally bicarbonate-free Ringer's for 40–60 min. Row 3 is the mean percent decrease in J_V induced by bicarbonate removal.

Effects of Ouabain on J_V

In many epithelia, fluid transport is dependent on the activity of the Na pump (Reuss et al., 1979). It has been previously demonstrated that bullfrog RPE has a ouabain-sensitive, electrogenic Na-K pump on the apical, but not the basal, membrane (Miller and Steinberg, 1977*a*, 1982; Miller et al., 1978; Oakley et al., 1978; Riley et al., 1978; Ostwald and Steinberg, 1980; Bok, 1982). Depending on the mechanism(s) by which the operation of the pump is coupled to fluid transport, there are several possible outcomes of an experiment that involves pump inhibition by ouabain. For example, since the pump is electrogenic, there is a net cation (Na) flux out of the cell through the pump, and this movement of Na, along with the obligatory anions, could osmotically drive fluid across the apical membrane in the secretory direction (choroid to retina). This postulated secretory flow would oppose and reduce the magnitude of the net observed retina-to-choroid fluid movement. Inhibition of the pump with ouabain is then expected to increase the net fluid absorption. On the other hand, the observed

fluid absorption might be coupled to an ion transport mechanism that depends on the Na gradient across the apical or basal membrane(s), and thus inhibition of the Na pump would slowly dissipate the Na gradient (Miller et al., 1978) and reduce fluid transport.

Fig. 5 is a summary of seven experiments in which 0.1 mM ouabain was mixed into the apical bathing solution (100% J_V corresponds to 4.7 ± 0.5 μl/cm^2·h). After 10 min exposure to ouabain, there was no significant change in J_V, but after 1 h, the fluid absorption rate dropped by 50%. In comparison, the

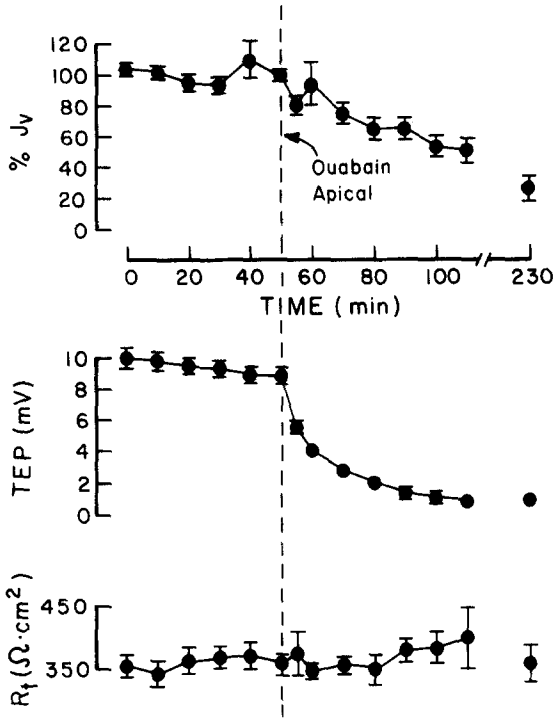

FIGURE 5. Effect of ouabain on J_V, TEP, and R_t across the RPE-choroid. Each point and vertical bar represents the mean ± SEM of four to seven experiments. J_V has been normalized to percent initial rate; the mean initial J_V was 4.7 ± 0.5 μl/cm^2·h (mean ± SEM).

spontaneous rate of decrease in J_V is only 16.4% (Fig. 3). After 3 h of exposure to ouabain, J_V dropped to 1.1 μl/cm^2·h (n = 4). The fact that the fluid absorption rate was never observed to rise seems to rule out the possibility that fluid transport is directly coupled to the activity of the Na-K pump. The slow decline in J_V is, however, consistent with the idea that fluid transport is dependent on the Na and/or K gradient across the apical or basal membranes.

Fig. 5 shows that ouabain had its usual effect on R_t and TEP (Miller et al., 1978). R_t increased slightly as a result of ouabain administration in five of the tissues, but in the other two there was no significant change. The TEP decreased

to 0.8 ± 0.3 mV after 60 min exposure to ouabain (t = 110 min), and after 3 h (t = 230 min) the TEP was 0.9 ± 0.2 mV (n = 4), a value significantly different from zero ($P < 0.001$). At this time, the pump was probably fully inhibited (Miller and Steinberg, 1982). The nonzero value of TEP may indicate that the RPE contains other active transport systems that drive fluid across the tissue. One such system that has been inferred from previous experiments depends on external bicarbonate ion (Steinberg and Miller, 1979; Miller and Farber, 1984). Of course, the nonzero TEP might also arise from diffusion potentials across the cell membranes generated by ions that are not yet in equilibrium.

Effects of cAMP on J_V

In a variety of epithelia, the regulation of ion and fluid transport is mediated by changes in the intracellular level of cAMP (Rasmussen, 1981). In the short-

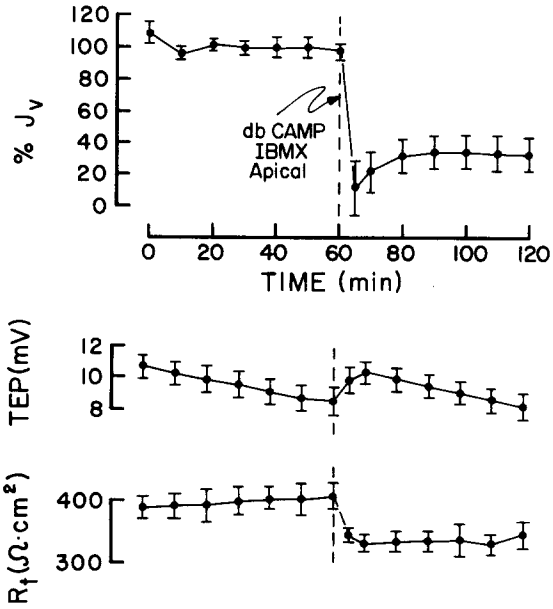

FIGURE 6. Effect of dbcAMP and IBMX on J_V, TEP, and R_t across the RPE-choroid. Each point and vertical bar represents the mean ± SEM for four to six experiments. J_V has been normalized to percent initial rate; the mean initial J_V was 5.5 ± 1.5 $\mu l/cm^2 \cdot h$ (mean ± SEM).

circuited bullfrog RPE, 1 mM cAMP or the same concentration of its analogue, dbcAMP, caused an increase in the choroid-to-retina flux of ^{22}Na and ^{36}Cl, but did not significantly affect the flux of these isotopes in the opposite direction (Miller and Farber, 1984). This cAMP-dependent NaCl secretion is opposite to the direction of fluid transport that is present across the resting tissue and therefore might cause a decrease in the fluid absorption rate.

Fig. 6 is a summary of six experiments in which 1 mM dbcAMP and 0.1 mM of the phosphodiesterase inhibitor IBMX were mixed into the apical bathing

solution (100% J_V corresponds to 5.5 $\mu l/cm^2 \cdot h$). This caused J_V to decrease to 16% of its initial value within 5 min; the decrease was followed by a rebound to a steady state that was 34% of the initial rate. In view of the possible effects of butyrate and/or IBMX on processes other than cAMP metabolism (Smith et al., 1979), we also investigated the effect of cAMP on fluid absorption by the RPE. Cyclic AMP (1 mM) added to the apical bathing solution produced changes in TEP and R_t that were similar to those induced by dbcAMP plus IBMX, but its effect on J_V was somewhat different: J_V decreased montonically to a steady state rate that was 39 ± 10% of the initial rate (n = 3), with no transient undershoot. The basis for this discrepancy is not understood at this time, but preliminary experiments indicate that the undershoot may be an artifact caused by a dbcAMP/IBMX-induced increase in choroidal thickness.

Fig. 6 shows that the addition of dbcAMP and IBMX to the solution bathing the apical membrane also resulted in characteristic changes in TEP and R_t (Miller and Farber, 1984). TEP increased to a peak of ~2 mV, which occurred ~10 min after the drug was first administered and then slowly declined at a rate not significantly different from the rate at which the TEP had declined before the treatment. Coinciding with the stimulation of the TEP was a decrease in R_t. R_t decreased ~75 $\Omega \cdot cm^2$ in the first 10 min after administration of the drugs and thereafter did not change significantly.

Ion Transport in the Open Circuit: Control and cAMP Treatment

In order to understand the ion transport processes that are responsible for net fluid transport and for the changes in fluid transport induced by cAMP, it is necessary to measure the net ionic fluxes in the open circuit. These open-circuit measurements give a more accurate picture of the in vivo movement of ions and water across the epithelium.

The results from 48 experiments on paired tissues are summarized in Tables II–IV. In the open circuit, there is a net absorption of ^{22}Na and ^{86}Rb (Tables III and IV, column 2) and a net secretion of ^{36}Cl (Table II, column 2). (It was previously shown that ^{86}Rb and ^{42}K are equivalent tracers for studying the movements of potassium across the RPE [Miller and Steinberg, 1982].) The effect of cAMP is to increase the secretion of NaCl (Tables II and III, column 3) and the absorption of K (Table IV, column 3).

Cyclic AMP also has a significant effect on the transepithelial potential and resistance. In all cases (Tables II–IV, row 4), TEP increased by 2–3 mV and R_t decreased by 40–60 $\Omega \cdot cm^2$. In the open circuit, the time courses of the cAMP-induced changes in unidirectional fluxes, TEP, and R_t were similar to those found under short-circuit conditions (compare Fig. 6 and Tables II–IV with Tables I–III in Miller and Farber, 1984).

DISCUSSION

In the present study, a modified version of a capacitance probe technique has been used to measure fluid transport across the isolated RPE-choroid of the bullfrog (Wiedner, 1976; Wright et al., 1977; van Os et al., 1979). There are two main technical difficulties in making these measurements. First, the RPE-

TABLE II

Cyclic AMP-induced Changes in ^{36}Cl Transport

Retina to choroid (A → B)	Control	cAMP	Difference
Unidirectional flux (μeq/cm^2·h)	0.92±0.04 (8)	0.92±0.06 (8)	0.00±0.04 (steady state)
TEP (mV)	8.9±0.75	—	+2.36±0.29* (peak)
R_t (Ω·cm^2)	273±8.4	—	−46.2±6.3* (peak)
Choroid to retina (B → A)	**Control**	**cAMP**	**Difference**
Unidirectional flux (μeq/cm^2·h)	1.37±0.16 (8)	1.95±0.20 (8)	+0.58±0.08* (steady state)
TEP (mV)	9.4±1.0	—	+2.03±0.35* (peak)
R_t (Ω·cm^2)	273±1.4	—	−41.3±5.6* (peak)
Net flux (μeq/cm^2·h)	0.45 (B → A)‡	1.03 (B → A)§	0.58

The values in each column are means ± SEM. In columns 2 and 3, the numbers in parentheses refer to the number of tissues. The magnitude and direction of the net flux, before and after cAMP, are given in columns 2 and 3 (bottom). The net transport is the algebraic difference between the retina-to-choroid and the choroid-to-retina unidirectional fluxes. In the open circuit, the net chloride flux is in the choroid-to-retina direction, before and after cAMP (columns 2 and 3, bottom). In both cases, the magnitude of this flux difference is statistically different from zero (‡$P = 0.013$; §$P < 0.001$; paired t test). The cAMP-induced changes in resistance, TEP, and choroid-to-retina unidirectional flux (column 4) are all statistically significant (*$P < 0.001$; paired t test).

choroid, made up of a single layer of cells plus the choroid, is fragile and difficult to mount in a chamber without causing some edge damage (Miller and Steinberg, 1977*a*, *b*). The second difficulty, not unrelated to the first, is the relatively small surface area available for study, ~0.1 cm^2. In order to detect a fluid transport rate of 10 μl/cm^2·h, a technique is required that could measure an absolute flow rate of 17 nl/min.

TABLE III

Cyclic AMP-induced Changes in ^{22}Na Transport

Retina to choroid (A → B)	Control	cAMP	Difference
Unidirectional flux (μeq/cm^2·h)	2.31±0.12 (8)	2.22±0.09 (8)	−0.09±0.05 (steady state)
TEP (mV)	9.20±0.61	—	+2.60±0.20* (peak)
R_t (Ω·cm^2)	259±7.7	—	−40.6±4.9* (peak)
Choroid to retina (B → A)	**Control**	**cAMP**	**Difference**
Unidirectional flux (μeq/cm^2·h)	1.77±0.09 (8)	2.36±0.08 (8)	+0.59±0.08* (steady state)
TEP (mV)	8.9±0.62	—	+2.40±0.20* (peak)
R_t (Ω·cm^2)	286±9.1	—	−45.5±4.2* (peak)
Net flux (μeq/cm^2·h)	0.54 (A → B)‡	0.14 (B → A)§	0.68

In the open circuit, before the application of cAMP, the net Na flux is in the retina-to-choroid direction and the magnitude of this flux difference is significantly different from zero (column 2, bottom; ‡$P <$ 0.001; unpaired t test). After addition of cAMP, the direction of net flux is reversed (column 3, bottom) but this value is not significantly different from zero (§$P = 0.74$; unpaired t test). The cAMP-induced changes in resistance, TEP, and choroid-to-retina unidirectional flux (column 4) are all statistically significant (*$P < 0.001$; paired t test).

In order to detect small volume flows across an epithelium using this technique, it is important to reduce significantly the baseline volume changes that can occur from absorption by the chamber walls or from evaporation of the Ringer's in the Teflon cups (Materials and Methods, Fig. 1). The material and the design of the present chamber helped minimize these background volume changes. Consequently, we were able to determine the magnitude of transepithelial fluid flow with a resolution of ~1 nl/min.

The present experiments demonstrate that the isolated RPE-choroid of the bullfrog transports fluid from the retinal to the choroidal side at a rate of ~10 nl/min (4–6 $\mu l/cm^2 \cdot h$). The latter range is comparable to that of other epithelia of the frog, such as the gallbladder and the choroid plexus (Frederiksen and Rostgaard, 1974; Wright et al., 1977). This study also shows that net fluid

TABLE IV

Cyclic AMP-induced Changes in K (^{86}Rb) Transport

Retina to choroid (A → B)	Control	cAMP	Difference
Unidirectional flux ($\mu eq/cm^2 \cdot h$)	0.16±0.02 (3)	0.36±0.04 (8)	+0.20±0.03* (steady state)
TEP (mV)	9.60±0.68	—	+3.25±0.23* (peak)
R_t ($\Omega \cdot cm^2$)	231±16.1	—	−45.5±56* (peak)
Choroid to retina (B → A)	**Control**	**cAMP**	**Difference**
Unidirectional flux ($\mu eq/cm^2 \cdot h$)	0.02±0.002. (8)	0.06±0.009 (8)	+0.04±0.008* (steady state)
TEP (mV)	8.5±0.86	—	+3.09±0.20* (peak)
R_t ($\Omega \cdot cm^2$)	249±16.1	—	−42±44* (peak)
Net flux ($\mu eq \cdot cm^2 \cdot h$)	0.14 (A → B)‡	0.30 (A → B)‡	0.16

In the open circuit, the net K transport is in the retina-to-choroid direction, before and after cAMP (columns 2 and 3, bottom). In both cases, the magnitude of this flux difference is significantly different from zero (‡$P < 0.001$; unpaired t test). The cAMP-induced changes in resistance, TEP, and unidirectional flux (column 4) are all statistically significant (*$P < 0.001$; paired t test).

absorption is: (*a*) abolished by the mitochondrial uncoupler DNP; (*b*) dependent on HCO_3 concentration and/or pCO_2 in the bulk solutions; (*c*) not directly coupled to the activity of the Na-K pump; (*d*) significantly reduced by exogenous cAMP; and (*e*) most likely generated primarily by the active absorption of bicarbonate, the passive and active movements of K, and the passive absorption of Na. The inhibitory effect of cAMP on fluid absorption is caused by the stimulation of a secretory flux of Na and Cl.

Metabolic Inhibition of Fluid Transport Across the RPE

Net fluid movement across the RPE occurs in the absence of external transepithelial osmotic and hydrostatic driving forces. In fact, one of the criteria that demonstrate the viability of the preparation requires that there be net fluid absorption against a small hydrostatic pressure gradient (Materials and Methods).

The driving force for fluid transport depends on active transport processes that are generated within the RPE cells (Miller and Steinberg, 1977*a*, 1982; Miller et al., 1978). This conclusion is supported by the finding that fluid absorption is abolished by the mitochondrial inhibitor DNP. Because of its lack of specificity, however, DNP could bring about the cessation of fluid tranpsort by some means other than limiting the availability of ATP. For example, DNP could act as a proton ionophore on the cell membranes and thereby disrupt ion transport processes to which fluid movement may be linked. Of course, these ion transport processes are ultimately linked to metabolic processes within the cells. Fluid transport is also abolished by blocking glycolytic and oxidative metabolism with Na azide plus iodoacetamide or anoxia plus iodoacetamide.

The Na-K Pump

The time course and the direction of the ouabain-induced change in J_V strongly suggest that the apical membrane Na-K electrogenic pump is not directly coupled to J_V. It was previously demonstrated that ouabain depolarizes the apical membrane potential (V_A) and decreases the TEP in two phases (Miller et al., 1978). The initial phase, complete within 2–3 min, is due to the removal of the electrogenic pump component of V_A (and TEP). The second phase of the membrane depolarization, which occurs over hours, is due to the dissipation of ionic gradients across the apical and basolateral membranes. The time scale in Fig. 6 (middle panel) does not allow one to discern these two phases, but the data clearly show that ouabain caused a rapid decrease in TEP. In contrast, there was no appreciable ouabain-induced change in J_V over the first 10 min, but after 1 h J_V had decreased by 50%. The slow decrease in J_V is probably due to the inhibition of ionic transport mechanisms (e.g., bicarbonate transport) that depend on the Na,K electrochemical gradients. Most importantly, the fact that fluid is absorbed, not secreted, across this tissue makes it seem unlikely that the apical membrane Na-K pump is the major determinant of fluid transport.

Net Ion Fluxes and Fluid Transport During Control Conditions

As a first step toward identifying the mechanisms responsible for fluid absorption across the RPE, we measured, along with J_V, the open-circuit fluxes of ^{22}Na, ^{86}Rb (as a marker for K), and ^{36}Cl during control conditions and then after cAMP treatment. The direction and magnitude of these ion fluxes are summarized in Fig. 7. During control conditions, there is a net absorption (A $\rightarrow$ B) of Na and K at rates of 0.54 and 0.14 $\mu eq/cm^2 \cdot h$, respectively, and a net secretion (B $\rightarrow$ A) of chloride at a rate of 0.45 $\mu eq/cm^2 \cdot h$ (see also Tables II–IV, column 2). Therefore, for open-circuited tissues, the net cation flux of Na and K, 0.68 $\mu eq/cm^2 \cdot h$, is in one direction (retina to choroid), while net Cl flux is in the opposite direction.

Electroneutrality requires that the net current across an open-circuited epithelium be equal to zero. This constraint can be used to identify the counterions that move with Na, K, and Cl. The algebraic sum of the net "cation" fluxes (Na + K + Cl) is 1.13 $\mu eq/cm^2 \cdot h$ since, by definition, a net secretion of anions (Cl) can be replaced with an equivalent absorption of cations. This net "absorption"

of cations must be accompanied by an equal absorption of "anions." The divalent cations Mg^{++} and Ca^{++} can be ignored because their net fluxes are negligible compared with Na, K, and Cl (Miller and Steinberg, 1977*a*). The only other major ions in the bathing media are bicarbonate and hydrogen; therefore, the net "cation" absorption must be balanced by either net HCO_3^- absorption or net H^+ secretion or a combination of both. Because of the relatively large rate of fluid absorption, net bicarbonate absorption must significantly exceed net hydrogen secretion. This net transport must be active since it occurs against the electrochemical gradient of bicarbonate (TEP ≃ 10 mV, zero chemical gradient).

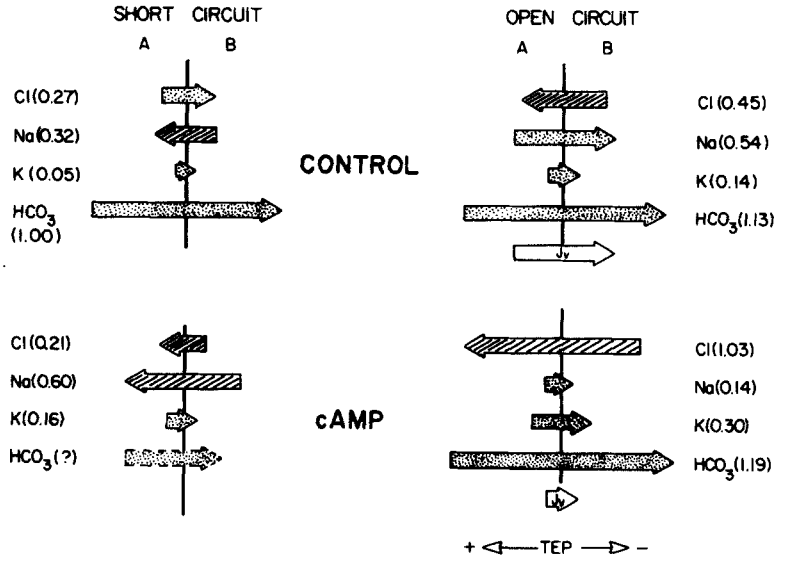

FIGURE 7. Summary of net fluxes under short-circuit and open-circuit conditions in control and cAMP-treated tissues. The magnitudes of the net fluxes (microequivalents per square centimeter per hour) are shown in parentheses. The retina-to-choroid net fluxes (A → B) are shown as stippled arrows and the choroid-to-retina net fluxes (B → A) are shown as cross-hatched arrows. The open arrows represent fluid absorption in the open circuit. Under control conditions, J_V = 5.5 μl/cm²·h, and in the cAMP-treated tissues, J_V = 1.8 μl/cm²·h. The TEP is apical side positive.

Thus, a major conclusion of this study is that active HCO_3 transport is the dominant driving force for fluid absorption across the RPE. This finding is consistent with our observations that J_V can be inhibited (≃70%) by removing bicarbonate and CO_2 from the external bathing solutions (Table I).

The measurements of ion fluxes in short-circuited tissues (Steinberg and Miller, 1979; Miller and Farber, 1984) indicate that a large fraction of the short-circuit current (0.6–1.0 μeq/cm²·h) is contributed by active bicarbonate absorption. In a variety of epithelia (Cohen, 1980; Norby et al., 1981; Fisher et al., 1981; Warnock and Eveloff, 1982), bicarbonate transport occurs as a result of Na-H and/or anion exchange, but in the RPE the nature and location of this transport system is unknown.

Effects of cAMP on Ion Fluxes and Fluid Transport

The present study shows that cAMP increased each of the B → A (choroid-to-retina) fluxes of Na and Cl by 0.65 μeq/cm^2·h, and also increased the A → B (retina-to-choroid) flux of K by 0.16 μeq/cm^2·h. These changes reduced the net absorption of cations (Na + K), increased the net secretion of anions (Cl), and produced a total "cation" absorption of 1.19 μeq/cm^2·h across the RPE. On the basis of electroneutrality, the net bicarbonate absorption across cAMP-treated tissues must also be 1.19 μeq/cm^2·h. This is very close to 1.13 μeq/cm^2·h, which was obtained under control conditions, and suggests that cAMP has relatively little effect on the bicarbonate transport system. Therefore, the main effect of cAMP on ion transport is the generation of a secretory flux of NaCl.

The cAMP-mediated changes in J_V are shown in Fig. 6. For comparison with those data, one can use the net fluxes of the actively transported ions, in the open circuit, to calculate J_V. The algebraic sum of all the net fluxes is given by $J_S = J_K$ (A → B) + J_{Na} (A → B) + J_{HCO} (A → B) − J_{Cl} (B → A), and using the values from Tables II–IV (columns 2 and 3), one obtains J_S = 1.36 μeq/cm^2·h for control tissues and J_S = 0.32 μeq/cm^2·h for cAMP-treated tissues. If we assume that ion and fluid transport across the RPE are isotonically coupled, then the equation $J_S/J_V = c$ can be used to calculate J_V (c is the total concentration of solute in the bathing solutions). Since the concentration of the bathing solution is 242.5 mM (Materials and Methods), the predicted J_V under control and cAMP conditions is 5.6 μl/cm^2·h and 1.3 μl/cm^2·h, respectively.

On the assumption of isotonic coupling, we would therefore expect cAMP to reduce J_V by 4.3 μl/cm^2·h. In Fig. 6 the observed control value of J_V (100%) is 5.5 μl/cm^2·h, which is reduced to 1.8 μl/cm^2·h in cAMP (a difference of 3.7 μl/cm^2·h). The agreement between the observed and predicted J_V is good, given the precision of the data and the fact that the flux and fluid measurements were made on two separate sets of tissues; it strongly supports the idea that the cAMP-induced NaCl secretion is coupled to fluid secretion.[2]

Directions and Pathways of Solute Movement

The magnitude and the direction of the net fluxes in the open circuit (present study) and the short circuit (Miller and Farber, 1984) differ, under control conditions, because of the TEP which exists across the tissue in open circuit. This "transport" potential is, of course, brought to zero by the short-circuit current. Although we cannot yet specify the pathways for fluid transport across the RPE, we can use the available transport information to indicate the major pathways for solute movement. A summary diagram of the short-circuit and open-circuit fluxes is shown in Fig. 7. The net ^{22}Na flux present in the short-

[2] If one combines all of the J_V data in Figs. 3–6, the overall average is 4.8 ± 0.34 μl/cm^2·h (mean ± SEM, n = 5). Using this value of J_V and J_S = 1.36 μeq/cm^2·h for control tissues (Tables II–IV, column 2), one obtains J_S/J_V = 283 ± 20 mM (mean ± SEM), which suggests that the absorbate may be somewhat hypertonic to the bathing solutions (c = 245.5 mM). If J_S/J_V = 283 mM, then the predicted J_V for control and cAMP-treated tissues would be 4.8 and 1.1 μl/cm^2·h, respectively. These values and their difference, 3.5 μl/cm^2·h, still agree well with the data in Fig. 6.

circuit state (0.32 μeq/cm^2·h, B → A) is reversed when the TEP is turned on (0.54 μeq/cm^2·h, A → B). The difference is mainly due to a large TEP-dependent increase in the retina-to-choroid (A → B) flux. Therefore, there is a net movement of Na across the tissue in the retina-to-choroid direction. Most of this net current probably flows through the paracellular shunt driven by the TEP because the flux is voltage dependent. In the cellular pathway, the Na conductance of the apical and basal membranes is small (Miller and Steinberg, 1977*b*), there is a very steep electrochemical gradient of 120–150 mV, which prevents Na exit across the basal membrane, and the Na-K pumps are localized to the apical membrane (Miller and Steinberg, 1982).

The direction of net K (^{86}Rb) flux is not reversed when the TEP is turned on; the net absorption of K is increased, by a factor of almost 3, because of a large TEP-dependent increase in the retina-to-choroid flux. Therefore, in this case it is likely that both pathways, paracellular and cellular, are utilized. The driving force in the paracellular pathway is the TEP. In the cellular pathway, the apical membrane Na-K pump allows K entry against its electrochemical gradient, while K exit is down an electrochemical gradient at the basal membrane (Miller and Steinberg, 1977*b*; Oakley et al., 1978).

The net ^{36}Cl flux in the short-circuit state (0.27 μeq/cm^2·h, A → B) is reversed to 0.45 μeq/cm^2·h (B → A) when the tissue is transporting in the open circuit. This difference is mainly due to a large TEP-dependent increase in the choroid-to-retina (B → A) flux. It should be noted that the direction of net Cl flux in the open circuit, choroid to retina, is opposite to that found in the short circuit. This suggests that a significant fraction of the open-circuit flux is driven across the paracellular shunt by the TEP (apical side positive).

Changes in the transcellular flux might also arise from TEP-dependent changes in membrane voltage or conductance that occur at the apical or basolateral membrane in the transition from short circuit to open circuit (TEP ≃ 10 mV). Although these changes are small, 3–4 mV hyperpolarization for the apical membrane and 6–7 mV depolarization for the basolateral membrane (S. S. Miller and R. H. Steinberg, unpublished observations), and the chloride conductances of the cell membranes are close to zero (Miller and Steinberg, 1977*b*), this possibility cannot be ruled out because no information is yet available about the driving force(s) for Cl (or bicarbonate) at the apical or basolateral membranes.

The net flux of HCO_3 (inferred) in the open circuit is in the retina-to-choroid direction against its electrochemical gradient. Therefore, this active HCO_3 absorption must occur via the cellular pathway.

Physiological Roles

In the intact eye, cAMP-mediated fluid absorption across the RPE may be an important mechanism for controlling the chemical milieu and the volume of the subretinal space (Introduction). This kind of mechanism, by altering photoreceptor function, could exert its influence beyond the subretinal space to the retina as a whole. In the photoreceptors, the absorption of a photon of light produces an electrical signal that electronically spreads toward the synaptic end of the cell. This signal is modified and amplified along the length of the receptor by a wide

variety of ionic and enzymatic mechanisms that depend on the chemical composition of the subretinal space (Capovilla et al., 1980). Therefore, any fluid transport-induced changes in the composition of the subretinal space could also influence the electrical activity of the more proximal retinal neurons.

In the human eye, there are a wide variety of pathologies that lead to the accumulation of fluid in the subretinal space. If not corrected, this condition usually leads to blindness. In the case of retinal detachments, the resorption of fluid from the subretinal space is commonly observed even in the presence of tears or holes in the retina. On the basis of such observations, it has been postulated that the RPE "actively" removes fluid from the subretinal space and helps promote a normal adhesion between the retina and the pigment epithelium, presumably by minimizing the distance between the photoreceptors and the PE cells (Gass, 1977; Zauberman, 1979; Marmor et al., 1980).

Solute-linked fluid transport across the RPE might also play a role in the overall fluid dynamics of the eye. In vertebrates, the intraocular pressure is kept constant by a balance between the fluid that enters the eye and the fluid that exits the eye. The exit pathways are mainly in the anterior chamber, but the present findings raise the question of whether the PE might also provide a significant pathway for the exit of intraocular fluid.

We are grateful to L. Reuss and E. Wright for their helpful comments during the preparation of this manuscript. We also wish to thank A. Halio and D. Joseph for expert technical assistance. It is our pleasure to thank D. Rehder for his help in the design and construction of the Kel-F chamber.

This research was supported by the National Eye Institute (EY 02205 to S.S.M.), the National Science Foundation (PCM 7722505 to T.E.M.), and Core Center Grant EY 03176. B.A.H. was supported by National Institutes of Health Training Grant GM 07379-06.

Received for publication 28 October 1983 and in revised form 4 January 1984.

REFERENCES

Bach, G., and E. R. Berman. 1971. Amino sugar containing compounds of the retina. I. Isolation and identification. *Biochim. Biophys. Acta.* 252:453–461.

Berman, E. R. 1969. Mucopolysaccharides (glycosaminoglycans) of the retina: identification, distribution, and possible biological role. *In* Fundamental Research Related to Retinal Detachment. E. B. Streiff, editor. S. Karger, Basel, New York. 8:5–13.

Bok, D. 1982. Autoradiographic studies on the polarity of plasma membrane receptors in retinal pigment epithelial cells. *In* IVth International Symposium on the Structure of the Eye. J. Hollyfield, editor. Elsevier/North-Holland, New York. 247–256.

Capovilla, M., L. Cervetto, and L. Torre. 1980. Effects of changing external potassium and chloride concentrations on the photoresponses of *Bufo bufo* rods. *J. Physiol. (Lond.).* 307:529–551.

Cohen, L. 1980. HCO-Cl exchange transport in the adaptive response to alkalosis by turtle bladder. *Am. J. Physiol.* 239:F167–F174.

Feeney, L. 1973. The interphotoreceptor space. II. Histochemistry of the matrix. *Dev. Biol.* 32:115–128.

Fischbarg, J., and G. Whittembury. 1978. The effect of external pH on osmotic permeability,

ion and fluid movement across the isolated frog skin. *J. Physiol. (Lond.)*. 275:403–417.

Fisher, R. S., B. E. Persson, and K. R. Spring. 1981. Epithelial cell volume regulation: bicarbonate dependence. *Science (Wash. DC)*. 214:1357–1359.

Frederiksen, O., and J. Rostgaard. 1974. Absence of dilated lateral intercellular spaces in fluid transporting frog gallbladder epithelium: direct microscopy observation. *J. Cell Biol.* 61:830–834.

Freeman, R. D. 1972. Oxygen consumption by the component layers of the cornea. *J. Physiol. (Lond.)*. 225:15–32.

Gass, J. D. M. 1977. Stereoscopic Atlas of Macular Diseases. C. V. Mosby Co., St. Louis, MO. 19–38.

Gold, G. H., and J. I. Korenbrot. 1980. Light induced calcium release by intact retinal rods. *Proc. Natl. Acad. Sci. USA*. 77:5557–5561.

Griff, E. R., and R. H. Steinberg. 1982. Origin of the light peak. *J. Physiol. (Lond.)*. 275:403–417.

House, C. R. 1974. Water Transport in Cells and Tissues. Edward Arnold, London. 390–470.

Hughes, B. A., S. S. Miller, and T. E. Machen. 1982. Fluid transport across the retinal pigment epithelium. *Fed. Proc.* 41:1351. (Abstr.)

Linsenmeier, R. A., A. A. Mines, and R. H. Steinberg. 1983. Effects of hypoxia and hypercaphia on the light peak and electroretinogram of the cat. *Invest. Ophthalmol. Visual Sci.* 24:37–46.

Linsenmeier, R. A., and R. H. Steinberg. 1982. Origin and sensitivity of the light peak in the intact cat eye. *J. Physiol. (Lond.)*. 331:653–673.

Marmor, M. F., A. S. Abdul-Rahim, and D. S. Cohen. 1980. The effect of metabolic inhibitors on retinal adhesion and subretinal fluid resorption. *Invest. Ophthalmol. Visual Sci.* 19:893–903.

Miller, S. S., and D. Farber. 1984. Cyclic AMP modulation of ion transport across frog retinal pigment epithelium. Measurements in the short-circuit state. *J. Gen. Physiol.* 83:853–874.

Miller, S. S., B. Hughes, and T. E. Machen. 1982. Fluid transport across the retinal pigment epithelium is inhibited by cyclic AMP. *Proc. Natl. Acad. Sci. USA*. 79:2111–2115.

Miller, S. S., and R. H. Steinberg. 1977*a*. Active transport of ions across the frog retinal pigment epithelium. *Exp. Eye Res.* 25:235–248.

Miller, S. S., and R. H. Steinberg. 1977*b*. Passive ionic properties of frog retinal pigment epithelium. *J. Membr. Biol.* 36:337–372.

Miller, S. S., and R. H. Steinberg. 1979. Potassium modulation of taurine transport across the frog retinal pigment epithelium. *J. Gen. Physiol.* 74:237–259.

Miller, S. S., and R. H. Steinberg. 1982. Potassium transport across the frog retinal pigment epithelium. *J. Membr. Biol.* 67:199–209.

Miller, S. S., R. H. Steinberg, and B. Oakley II. 1978. The electrogenic sodium pump of the frog retinal pigment epithelium. *J. Membr. Biol.* 44:259–279.

Noell, W. K. 1963. Cellular physiology of the retina. *J. Opt. Soc. Am.* 53:36–58.

Norby, L. H., D. Bethencourt, and J. H. Schwartz. 1981. Dual effect of carbonic anhydrose inhibitors on H transport by the turtle bladder. *Am. J. Physiol.* 240:F400–F405.

Oakley, B., II. 1977. Potassium and the photoreceptor-dependent pigment epithelial hyperpolarization. *J. Gen. Physiol.* 70:405–425.

Oakley, B., II, and D. G. Green. 1976. Correlation of light-induced changes in retinal extracellular potassium concentration with c-wave of the electroretinogram. *J. Neurophysiol.* 39:1117–1133.

Oakley, B., II, S. S. Miller, and R. H. Steinberg. 1978. Effects of intracellular potassium on the electrogenic pump of frog retinal pigment epithelium. *J. Membr. Biol.* 44:281–307.

Ostwald, T., and R. H. Steinberg. 1980. Localization of frog retinal pigment epithelium (Na, K)-ATPase. *Exp. Eye Res.* 31:351–360.

Rasmussen, H. 1981. Calcium and cAMP as Synarchic Messengers. John Wiley & Sons, New York. 1–370.

Reuss, L., E. Bello-Reuss, and T. P. Grady. 1979. Effects of ouabain on fluid transport and electrical properties of *Necturus* gallbladder. *J. Gen. Physiol.* 73:385–402.

Riley, M. V., B. S. Winkler, J. Benner, and E. M. Yates. 1978. ATPase activities in retinal pigment epithelium and choroid. *Exp. Eye Res.* 26:445–455.

Sidman, R. L. 1958. Histochemical studies on photoreceptor cells. *Ann. NY Acad. Sci.* 74:182–195.

Smith, P. A., F. F. Weight, and R. A. Lehne. 1979. Potentiation of Ca-dependent activation by theophylline is independent of cyclic nucleotide elevation. *Nature (Lond.).* 280:400–402.

Steinberg, R. H., and S. S. Miller. 1979. Transport and membrane properties of the retinal pigment epithelium. *In* The Retinal Pigment Epithelium. K. M. Zinn and M. F. Marmor, editors. Harvard University Press, Cambridge, MA. 205–225.

Steinberg, R. H., B. Oakley II, and G. Niemeyer. 1980. Light-evoked changes in $[K^+]$ in the retina of the intact cat eye. *J. Neurophysiol.* 44:897–921.

van Os, C. H., G. Wiedner, and E. M. Wright. 1979. Volume flows across gallbladder epithelium induced by small hydrostatic and osmotic gradients. *J. Membr. Biol.* 49:1–20.

Warnock, D., and J. Eveloff. 1982. NaCl entry mechanisms in the luminal membrane of the renal tubule. *Am. J. Physiol.* 242:1357–1359.

Welsh, M. J., J. H. Widdicombe, and J. A. Nadel. 1980. Fluid transport across the canine tracheal epithelium. *J. Appl. Physiol.* 49:905–909.

Wiedner, G. 1976. Method to detect volume flows in the nanoliter range. *Rev. Sci. Instrum.* 47:775–776.

Wright, E. M., G. Wiedner, and G. Rumrich. 1977. Fluid secretion by the frog choroid plexus. *Exp. Eye Res.* 25(Suppl):149–155.

Zauberman, H. 1979. Adhesive forces between the retinal pigment epithelium and the sensory retina. *In* The Retinal Pigment Epithelium. K. M. Zinn and M. F. Marmor, editors. Harvard University Press, Cambridge, MA. 192–204.